Higher order equivalent edge currents for fringe wave radar scattering by perfectly conducting polygonal plates

Breinbjerg, Olav

Published in:
I E E E Transactions on Antennas and Propagation

Link to article, DOI:
10.1109/8.204745

Publication date:
1992

Document Version
Publisher's PDF, also known as Version of record

Higher Order Equivalent Edge Currents for Fringe Wave Radar Scattering by Perfectly Conducting Polygonal Plates

Olav Breinbjerg, *Member, IEEE*

Abstract—**Two sets of higher order equivalent edge currents are introduced which, in combination, account for the first-, the second-, and part of the third-order edge diffraction caused by the fringe wave surface current induced on a perfectly conducting polygonal plate in a radar scattering configuration. The first set represents the fringe wave surface current excited by the incident plane wave at the leading edge on a finite incremental strip extending from the leading edge to the trailing edge. The second set represents the fringe wave surface current excited at the trailing edge by the incident leading edge fringe wave surface current on a finite incremental strip extending from the trailing edge to the third edge. The fringe wave surface current on the plate is approximated by the fringe wave surface current on half-planes appropriately conforming to the leading and trailing edges of the plate. For the second set of higher order equivalent edge currents, this requires a new model for the trailing edge fringe wave surface current. The proposed model will ensure that the normal component at the trailing edge of the approximate fringe wave surface current represented by the equivalent edge currents is zero. Both sets of higher order equivalent edge currents are defined to be placed at the leading edge, and since they contain very few singularities, these are numerically well behaved. Numerical results for the bistatic radar cross section of a square plate show that significant improvements over a first-order approach are obtained from the use of the proposed higher order equivalent edge currents.**

I. Introduction

THE method of equivalent edge currents (EEC's) constitutes a versatile high-frequency technique for the analysis of edge diffraction. The essential feature of the EEC method is that contributions from all edge points are explicitly taken into account. The diffraction process at each edge point is expressed in terms of electric and magnetic EEC's which, when employed in a line radiation integral along the circumference, yield the resulting field. There are three different types of EEC's which can be related to the total, the physical optics (PO), or the fringe wave (FW) surface currents induced on the scattering structure. Depending on which type of EEC is being employed in the line radiation integral, the resulting field will furnish an asymptotic approximation to the diffracted field, the PO-diffracted field, or the FW field. Accordingly, the three types of EEC's are referred to as geometrical theory of diffraction EEC's (GTDEEC's), physical optics EEC's (POEEC's), and physical theory of diffraction EEC's (PTDEEC's). Furthermore, the EEC's are termed first- or higher order according to whether the edge interaction is neglected or taken into account. Since the EEC method considers the contributions from all edge elements, its applicability does not—in contrast to the ray-optical diffraction techniques—rely on the existence of isolated stationary edge points, and consequently, the EEC method can be used for configurations where the ray-optical techniques cannot. Works on the theoretical aspects and applicability of the EEC method are numerous; however, fundamental ideas were developed and established by Millar [1], Mitzner [2], Michaeli [3], and Shore and Yaghjian [4].

The purpose of this paper is to present a new approach for the inclusion of the higher order edge diffraction in the EEC method. This approach applies to monostatic as well as bistatic radar scattering from perfectly conducting polygonal plates. Two sets of higher order PTDEEC's are formulated. The first set accounts for the first-order edge diffraction and part of the second-order edge diffraction. This set is derived through integration of the FW surface current excited at the leading edge of the scatterer by the incident plane wave along a finite, arbitrarily oriented incremental strip extending from the leading edge to the trailing edge. This FW surface current is approximated by that of a half-plane conforming to the leading edge. The second set accounts for the remaining part of the second-order edge diffraction and part of the third-order edge diffraction. This set is derived through integration of the FW surface current excited at the trailing edge by the incident FW surface current from the leading edge. The integration is carried out along a finite incremental strip oriented in the direction of the trailing edge Keller cone and extending from the trailing edge to the third edge. The essential step in the derivation of the second set of the higher order PTDEEC's consists in establishing an expression for the trailing edge FW surface current. This is achieved by noting that for a half-plane illuminated at grazing incidence, the FW surface current can be expressed in terms of the incident PO surface current at the edge. The FW surface current excited at the trailing edge is then ascribed the same functional dependence on the value of the incident leading edge FW surface current at

Manuscript received March 2, 1992; revised August 5, 1992.

The author is with the Electromagnetics Institute, Technical University of Denmark, 2800 Lyngby, Denmark.

IEEE Log Number 9204930.

0018-926X/92$03.00

the trailing edge. This new model will ensure that the component normal to the trailing edge of the approximate FW surface current represented by the PTDEEC's is zero, in agreement with physical considerations. Since both sets are based on finite incremental strips, the derived PTDEEC expressions contain very few singularities, and the fields produced by these are thus finite for most directions of incidence and observation. Both sets are defined to be placed at the leading edge. In this paper, only the calculation of the FW field is being considered. It is noted, however, that the PO field is rigorously obtained by applying the POEEC's [5], [6]. When the two sets of higher order PTDEEC's are added to the POEEC's, a combined set of EEC's is obtained which accounts for first-, second-, and part of the third-order edge diffraction. The scattered field is subsequently obtained by evaluation of one line radiation integral along the circumference of the scatterer. For the sake of completeness, this paper also includes a set of first-order PTDEEC's which accounts for the first-order edge diffraction. It is derived through integration of the FW surface current excited at the leading edge by the incident plane wave along an infinite, arbitrarily oriented incremental strip. This set is general in the sense that it comprises a number of previously reported expressions as special cases. The first- as well as the higher order PTDEEC's proposed in this paper pertain to flat plate scatterers since the derivation is based on Sommerfeld's half-plane solution [7]. However, the proposed procedure can be enhanced to also apply to polyhedral objects provided that the derivation of the PTDEEC's is based on the solution for the wedge.

It should be noted that the proposed approach does not account for the surface currents caused by the corners of the scatterer. Furthermore, it applies, in a strict sense, only to scatterers with straight edges. For curved edges, the approximate FW surface current represented by the PTDEEC's does not, in general, closely approximate the actual FW surface current; this was shown by Shore and Yaghjian [8]. Nevertheless, numerical results for the circular disk [8], [9] reveal that good agreement can be achieved for the scattered field even in this case.

The outline of this paper will be as follows. In Section II, the coordinate systems employed to specify the scattering configuration and the EEC's are introduced; furthermore, some previous works on higher order EEC's are discussed, and the half-plane surface current is given. In Section III, the set of general first-order PTDEEC's is presented. Section IV deals with the first set of higher order PTDEEC's. In Section V, the second set of higher order PTDEEC's is derived on the basis of the new expression for the trailing edge FW surface current. Section VI contains numerical results for a square plate configuration; first-order EEC results, higher order EEC results, and MOM results are compared.

II. Background

The radar scattering configuration is specified as follows. The scatterer is an infinitely thin, perfectly conducting, flat, polygonal plate residing in the xy plane of a rectangular (x, y, z) coordinate system with a spherical (r, θ, ϕ) coordinate system associated in the usual manner. Superscript "i" designates parameters relating to the incident field. The normal vector on the illuminated surface is denoted by $\hat{n}$ and it coincides with $\hat{z}$. The observation point is at infinity, and the direction of observation $\hat{r}$ is thus independent of the position on the scatterer. The incident field is a time-harmonic, linearly polarized, homogeneous plane wave. The time factor $\exp(j\omega t)$ is suppressed, and the incident electric and magnetic fields $\bar{E}^i$ and $\bar{H}^i$ are thus given by

$$\bar{E}^i(\bar{r}) = \bar{E}_0^i \exp\left(-jk\hat{k}\cdot\bar{r}\right) \tag{1}$$

$$\bar{H}^i(\bar{r}) = \bar{H}_0^i \exp\left(-jk\hat{k}\cdot\bar{r}\right) \tag{2}$$

wherein $\bar{E}_0^i$ and $\bar{H}_0^i$ are constant amplitude vectors, k is the free-space propagation constant, and $\hat{k}$ is the propagation vector:

$$\hat{k} = -\left(\hat{x}\sin\theta^i\cos\phi^i + \hat{y}\sin\theta^i\sin\phi^i + \hat{z}\cos\theta^i\right). \tag{3}$$

Based on the known behavior of the half-plane surface current (see later), the establishment of the high-frequency FW surface current on the scatterer can be regarded as taking place in the manner depicted in Fig. 1 wherein the octagon represents an arbitrary flat, polygonal plate. When the plane wave is incident on an edge point A, a FW surface current is excited here. This surface current propagates away from the edge in the direction defined by the intersection of the plate and the Keller cone pertinent to the edge point A. In the following, this edge point being illuminated by the plane wave is referred to as the *leading edge point*, and the excited FW surface current is referred to as the *leading edge FW surface current*. This leading edge FW surface current propagates until it is intercepted by another edge point B, henceforth referred to as the *trailing edge point*. The diffraction taking place here in turn excites a *trailing edge FW surface current* which propagates along the intersection of the plate and the Keller cone pertinent to the trailing edge point B until a *third edge point C* is reached. In principle, this process continues indefinitely; however, due to the fading of the surface current amplitude, the successive diffractions become less and less significant. Obviously, all edge points are leading since the entire circumference is illuminated by the incident plane wave. However, all edge points are not necessarily also trailing as they are not all illuminated by a surface current excited at another edge point. The *leading edge incremental strip* and the *trailing edge incremental strip* are defined as the strips of infinitesimal width extending from the edge elements at the leading and trailing edge points, respectively.

A local edge coordinate system is introduced to describe the scattering configuration with respect to an arbitrary edge point on the scatterer. With $\hat{t}_l$ being the leading edge tangent unit vector, the local edge coordinate system at the leading edge point is specified as

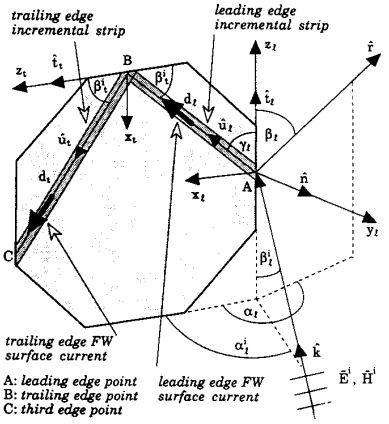

Fig. 1. The establishment of the high-frequency FW surface current on a polygonal plate illuminated by a plane wave, and the local leading and trailing edge coordinate systems.

follows (see Fig. 1). A rectangular (x_l, y_l, z_l) coordinate system is employed so that $\hat{z}_l$ and $\hat{y}_l$ coincide with $\hat{t}_l$ and $\hat{n}$, respectively. Furthermore, a rectangular (x_t, y_t, z_t) coordinate system is employed at the trailing edge point so that $\hat{z}_t$ and $\hat{y}_t$ coincide with the trailing edge tangent unit vector $\hat{t}_t$ and $\hat{n}$, respectively. In the leading edge coordinate system, the four angles α_l^i, β_l^i, α_l, and β_l are introduced to specify the directions of incidence and observation:

$$\alpha_l^i = \arctan\left(\hat{k}\cdot\hat{y}_l/\hat{k}\cdot\hat{x}_l\right), \qquad 0 \le \alpha_l^i \le \pi \tag{4}$$

$$\beta_l^i = \arccos\left(\hat{k}\cdot\hat{z}_l\right), \qquad 0 \le \beta_l^i \le \pi \tag{5}$$

$$\alpha_l = \arctan\left(\hat{r}\cdot\hat{y}_l/\hat{r}\cdot\hat{x}_l\right), \qquad 0 \le \alpha_l \le 2\pi \tag{6}$$

$$\beta_l = \arccos\left(\hat{r}\cdot\hat{z}_l\right), \qquad 0 \le \beta_l \le \pi. \tag{7}$$

The direction $\hat{u}_l$ of the leading edge incremental strip forms an angle γ_l with the leading edge tangent unit vector $\hat{t}_l$. It is noted that the leading edge incremental strip does not necessarily have to be oriented along the intersection of the plate and the Keller cone, in which case γ_l would equal β_l^i. The distance along the leading edge incremental strip from the leading edge point is denoted by u_l, and the length of the finite leading edge incremental strip, i.e., the distance between the leading and trailing edge points, is d_l. The parameters $\hat{u}_t$, u_t, and d_t are defined in an analogous manner for the trailing edge incremental strip, as also indicated in Fig. 1. The angle between the trailing edge incremental strip and the trailing edge is equal to the angle between the leading edge incremental strip and the trailing edge:

$$\beta_t^i = \arccos\left(\hat{u}_l\cdot\hat{z}_t\right), \qquad 0 \le \beta_t^i \le \pi. \tag{8}$$

A detailed review examining and comparing several works on theoretical developments and practical applications of the EEC method is given elsewhere [9]; in the following, only reported works on higher order EEC's will be discussed.

Prior to 1987, such works were reported by Millar [10], [11], Burnside and Peters [12], Knott and Senior [13], Sikta [14], and Wang and Medgyesi-Mitschang [15]. These works possess some common features. First, they all concern GTDEEC's. Second, the incident field exciting the higher order GTDEEC's at a given edge point is found as the field caused by the first-order GTDEEC's along all other parts of the circumference. This incident field is calculated either through an explicit integration [13], [15] employing a line radiation integral or through an implicit integration [10]–[12], [14] employing the stationary phase formula or UTD [16]. Third, being based on ray-optics, these GTDEEC's only consider three of the four angles $(\alpha^i, \beta^i, \alpha, \beta)$ specifying the directions of incidence and observation, whereas all four angles are needed at nonstationary edge points where β and β^i differ.

In 1987, Michaeli [17] derived a set of second-order PTDEEC's. These complement his first-order PTDEEC's [18] which represent the leading edge FW surface current on an incremental strip extending to infinity in the direction specified by the intersection of the scatterer and the Keller cone. The error of the first-order PTDEEC's, constituted by the part of the incremental strip extending beyond the actual scatterer, is cancelled by simultaneously applying the second-order PTDEEC's, representing the leading edge FW surface current on the extending part of the incremental strip, at the trailing edge of the scatterer. Michaeli's approach takes into account only part of the second-order edge diffraction since the diffraction process at the trailing edge is not entirely included; it is not ensured that the approximate FW surface current component perpendicular to the trailing edge is zero.

In 1989, Shore and Yaghjian [8] derived a set of incremental length diffraction coefficients (ILDC's) relating to a finite incremental strip. These ILDC's are to be applied at the leading edge and used instead of the first-order ILDC's [4]. Furthermore, the inclusion of the diffraction at the trailing edge was addressed by considering the behavior of the half-plane surface current. Assuming that the direction of incidence is close to edge-on $(\alpha^i \approx \pi)$ and that the distance from the edge is large, some terms of the surface current can be neglected. The total surface current can then be expressed as the PO surface current multiplied by a factor depending on the direction of incidence, the direction of the incremental strip, and the distance from the edge. The same factor is then applied to the ILDC's at the trailing edge of the actual scatterer.

In 1990, Ivrissimtzis [19] introduced a set of second-order PTDEEC's to be placed at the trailing edge. These equal Michaeli's first-order PTDEEC's excited by the spectrum of inhomogeneous plane waves representing the field diffracted from the leading edge. The field diffracted at the trailing edge is then expressed as a double integral; one is the integral along the trailing edge, while the other is the integral over the spectral components of the second-order PTDEEC's. The former integral is evaluated analytically. The latter integral is evaluated asymptotically, and the two leading terms are retained. The first of

these equals Michaeli's first-order PTDEEC's excited by the UTD ray-optical field from the leading edge, while the second accounts for slope diffraction. Since Michaeli's first-order PTDEEC's represent the FW surface current on an infinite incremental strip, Ivrissimtzis' approach implies that there are surface currents outside the actual scatterer, and these can cause errors for directions of observation close to the plane of the scatterer [9].

Recently, Ufimtsev [20] reported an approach formulated in terms of elementary edge waves (EEW's). The diffraction at the trailing edge is expressed as the sum of two terms. The first is the field generated by the first-order EEW's placed at the trailing edge, with the incident field taken as a ray-optical field diffracted at the leading edge. The second, a slope diffraction term, is expressed by EEW's employed at the trailing edge and determined as the derivatives of the first-order EEW's with respect to the direction normal to the surface of the scatterer. Ufimtsev's approach is also based on infinite incremental strips, and thus introduces surface currents outside the actual scatterer.

Since the derivation of the PTDEEC's, in subsequent sections, is based on the solution to the half-plane scattering problem, this configuration is considered in the following (see Fig. 2). The local edge coordinate system is applied at an arbitrary edge point (the subscripts on the coordinates are omitted since only one edge is involved). The incident plane wave is given by (1)–(2). From Sommerfeld's solution [7] for the total field, the PO and FW surface currents along the incremental strip forming an angle γ with the half-plane edge are found to be

$$J_x^{\mathrm{po}}(u) = 2\left(\bar{H}_0^i \cdot \hat{t}\right) \exp\left(jku(\sin\gamma \sin\beta^i \cos\alpha^i - \cos\gamma\cos\beta^i)\right) \quad (9)$$

$$J_z^{\mathrm{po}}(u) = 2\left(\frac{1}{\zeta}\left(\bar{E}_0^i \cdot \hat{t}\right)\frac{\sin\alpha^i}{\sin\beta^i} - \left(\bar{H}_0^i \cdot \hat{t}\right)\frac{\cos\beta^i\cos\alpha^i}{\sin\beta^i}\right) \cdot \exp\left(jku(\sin\gamma\sin\beta^i\cos\alpha^i - \cos\gamma\cos\beta^i)\right) \quad (10)$$

$$J_x^{\mathrm{fw}}(u) = -\left(\bar{H}_0^i \cdot \hat{t}\right)4\frac{e^{j\pi/4}}{\sqrt{\pi}}F\left(\sqrt{2ku\sin\gamma\sin\beta^i}\cos\frac{\alpha^i}{2}\right) \cdot \exp\left(jku(\sin\gamma\sin\beta^i\cos\alpha^i - \cos\gamma\cos\beta^i)\right) \quad (11)$$

$$J_z^{\mathrm{fw}}(u) = \left(\left(\bar{H}_0^i \cdot \hat{t}\right)\frac{\cos\beta^i\cos\alpha^i}{\sin\beta^i} - \frac{1}{\zeta}\left(\bar{E}_0^i \cdot \hat{t}\right)\frac{\sin\alpha^i}{\sin\beta^i}\right) \cdot 4\frac{e^{j\pi/4}}{\sqrt{\pi}}F\left(\sqrt{2ku\sin\gamma\sin\beta^i}\cos\frac{\alpha^i}{2}\right) \cdot \exp\left(jku(\sin\gamma\sin\beta^i\cos\alpha^i - \cos\gamma\cos\beta^i)\right) + \left(\frac{1}{\zeta}\left(\bar{E}_0^i \cdot \hat{t}\right)\sin\frac{\alpha^i}{2} - \left(\bar{H}_0^i \cdot \hat{t}\right)\cos\frac{\alpha^i}{2}\cos\beta^i\right) \cdot 4\frac{e^{-j\pi/4}}{\sqrt{\pi}}\frac{1}{\sin\beta^i\sqrt{2ku\sin\gamma\sin\beta^i}} \cdot \exp\left(-jku(\sin\gamma\sin\beta^i + \cos\gamma\cos\beta^i)\right). \quad (12)$$

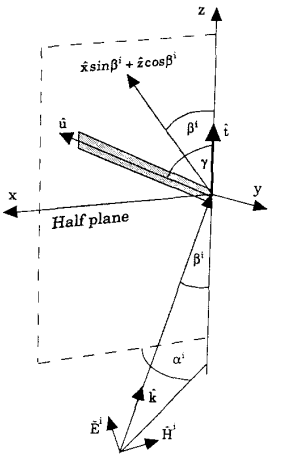

Fig. 2. Perfectly conducting half-plane illuminated by a plane wave. The shadowed region indicates the incremental strip starting at the edge point $z = 0$ and extending in the direction $\hat{u}$.

Herein, F denotes the Fresnel function:

$$F(x) = \int_x^\infty \exp(-jt^2)\,dt \quad (13a)$$

with

$$F(0) = \sqrt{\pi}\exp(-j\pi/4)/2 \quad (13b)$$

and

$$F(x) \sim \exp(-jx^2)/j2x, \qquad \text{for } x \to \infty. \quad (13c)$$

When the argument of the Fresnel function becomes large, use of the asymptotic representation (13c) shows that the FW surface current (11)–(12) is oriented in and propagating in the direction of the Keller cone: $\hat{x}\sin\beta^i + \hat{z}\cos\beta^i$. In the derivation of the second set of the higher order PTDEEC's, use will be made of the expressions for the half-plane FW surface current in the special case of grazing incidence ($\alpha^i = 0$). In this case, the induced FW surface current along the Keller cone ($\gamma = \beta^i$) can be expressed in terms of the PO surface current at the edge ($u = 0$):

$$J_x^{\mathrm{fw}}(u) = J_x^{\mathrm{po}}(0)\frac{-e^{j\pi/4}}{\sqrt{\pi}}F(\sqrt{2ku}\sin\beta^i) \cdot \exp[jku(\sin^2\beta^i - \cos^2\beta^i)] \quad (14)$$

$$J_z^{\mathrm{fw}}(u) = J_z^{\mathrm{po}}(0)\frac{-2e^{j\pi/4}}{\sqrt{\pi}} \cdot \left\{F(\sqrt{2ku}\sin\beta^i) - \frac{e^{-j2ku\sin^2\beta^i}}{j\sqrt{2ku}\sin\beta^i}\right\} \cdot \exp[jku(\sin^2\beta^i - \cos^2\beta^i)]. \quad (15)$$

III. First-Order PTDEEC's

In the EEC method, the asymptotic approximation to the FW field is found by evaluating a line radiation

integral over PTDEEC's along the circumference of the scatterer, i.e.,

$$\bar{E}^{\text{fw}} \sim jk\int_0^L \left[\zeta\hat{r}\times(\hat{r}\times\hat{t})I^{\text{ptd}} + \hat{r}\times\hat{t}M^{\text{ptd}}\right]\frac{e^{-jkR}}{4\pi R}\,dl. \tag{16}$$

Herein I^{ptd} and M^{ptd} are the electric and magnetic PTDEEC's, respectively, ζ is the free-space impedance, l denotes the arc length along the circumference of total length L, and R is the distance from the element of integration to the observation point. By identifying the expression (16) with an expression for the FW field obtained by an asymptotic reduction of the surface radiation integral over the induced FW surface current, Michaeli [3], [18] established the relations which express the PTDEEC's in terms of the induced FW surface current on the scatterer. The FW surface current on the scatterer was then approximated by the FW surface current on a canonical structure (the wedge) conforming to the actual scatterer at the edge point in question; for the flat plate, the canonical structure is the half-plane. Based on Michaeli's work, the half-plane first-order PTDEEC's $(I_l^{\text{ptd}}, M_l^{\text{ptd}})$ can thus be expressed as

$$I_l^{\text{ptd}} = \frac{|\hat{u}_l\times\hat{t}_l|}{|\hat{r}\times\hat{t}_l|^2}\hat{r}\cdot(\hat{t}_l\times\hat{r}) \times\int_0^\infty \bar{J}_l^{\text{fw}}(u_l)\exp(jk\hat{r}\cdot\hat{u}_l u_l)\,du_l \tag{17}$$

$$M_l^{\text{ptd}} = \zeta\frac{|\hat{u}_l\times\hat{t}_l|}{|\hat{r}\times\hat{t}_l|^2}\hat{t}_l\cdot\hat{r}\times\int_0^\infty \bar{J}_l^{\text{fw}}(u_l)\exp(jk\hat{r}\cdot\hat{u}_l u_l)\,du_l. \tag{18}$$

Hence, the first-order PTDEEC's are found through an integration of the half-plane FW surface current along an incremental strip starting at the edge and extending to infinity in the direction $\hat{u}_l$. The expressions (17)–(18) differ from those of Michaeli [18] in two aspects. First, Michaeli fixed the orientation of the incremental strip in the direction of the Keller cone, i.e,. $\hat{u}_l = \hat{x}_l\sin\beta_l^i + \hat{z}_l\cos\beta_l^i$. In the expressions above, the direction is not fixed, and upon evaluation of the integrals, this direction will thus appear parametrically in the explicit expressions for the PTDEEC's. Second, in Michaeli's expressions, the upper limit for the integral is absent, thus implying that only the lower end point contribution of the integral should be considered. However, for the half-plane FW surface current, the final expressions are the same whether the lower end point contribution is extracted using standard asymptotic techniques or the integration is carried out explicitly to infinity. Since the singularities of the PTDEEC's can be explained by realizing that the PTDEEC's represent the FW surface current on an infinite incremental strip, it seems appropriate to indicate this in the integral expressions (17)–(18). It is noted that Michaeli in his 1986 work on POEEC's [21] did employ an arbitrary strip direction, and consequently derived POEEC expressions containing the strip direction as a parameter.

Upon insertion of the half-plane FW surface current (11)–(12) in the integral expressions for the first-order PTDEEC's (17)–(18), the following explicit expressions are found:

$$I_l^{\text{ptd}} = \left(\bar{E}^i\cdot\hat{t}_l\right)\frac{2\sqrt{2}}{jk\zeta}\frac{\sin\frac{\alpha_l^i}{2}}{(\sin\beta_l^i)^{3/2}} \cdot\frac{1}{\sqrt{\sin\beta_l^i-\nu_l}+\sqrt{2\sin\beta_l^i}\cos\frac{\alpha_l^i}{2}} + \left(\bar{H}^i\cdot\hat{t}_l\right)\frac{2j}{k}\frac{1}{\sin^2\beta_l^i}\left[\cos\beta_l^i + \frac{1}{\sqrt{\sin\beta_l^i-\nu_l}}\cdot\frac{\nu_l\cos\beta_l^i-\sin^2\beta_l^i\cot\beta_l\cos\alpha_l}{\sqrt{\sin\beta_l^i-\nu_l}+\sqrt{2\sin\beta_l^i}\cos\frac{\alpha_l^i}{2}}\right] \tag{19}$$

$$M_l^{\text{ptd}} = \left(\bar{H}^i\cdot\hat{t}_l\right)\frac{2\zeta}{jk}\frac{\sin\alpha_l}{\sin\beta_l}\frac{1}{\sqrt{\sin\beta_l^i-\nu_l}} \cdot\frac{1}{\sqrt{\sin\beta_l^i-\nu_l}+\sqrt{2\sin\beta_l^i}\cos\frac{\alpha_l^i}{2}} \tag{20}$$

with

$$\nu_l = \sin\beta_l\cos\alpha_l + \cot\gamma_l(\cos\beta_l-\cos\beta_l^i) \tag{21}$$

and

$$\sqrt{\sin\beta_l^i-\nu_l} = -j\sqrt{|\sin\beta_l^i-\nu_l|} \quad \text{for } (\sin\beta_l^i-\nu_l)<0. \tag{22}$$

These PTDEEC's comprise previously reported expressions as special cases: by orienting the incremental strip perpendicular to the edge ($\gamma_l = 90°$), the EEC analogs of the ILDC's introduced by Mitzner [2] are recovered. If the incremental strip is oriented along the Keller cone ($\gamma_l = \beta^i$), the Michaeli PTDEEC's [18] are found. If the incremental strip is oriented along the projection onto the half-plane of the difference between the directions of observation and the Keller cone, the PTDEEC's reported recently by Ando *et al.* [22] are retrieved. It is emphasized that for numerical calculations, the incremental strip must be oriented in accordance with Michaeli's proposal since the FW surface current propagates in the direction of the Keller cone. The advantage of the generality of the expressions (19)–(20) is thus more conceptual than practical. It is observed from (21) that for edge stationary points where the polar angles of incidence and observation are equal ($\beta_l = \beta_l^i$), the PTDEEC's (19)–(20) are independent of the orientation of the infinite incremental strip

specified by the angle γ_l. Finally, it is noted that expressions for ILDC's based on an arbitrary direction of the infinite incremental strip were reported by Shore and Yaghjian [4]; thus, the expressions (19)–(20) constitute the EEC analogs of their ILDC expressions.

IV. First Set of Higher Order PTDEEC's

The first set of the higher order PTDEEC's (I_{12}^{ptd}, M_{12}^{ptd}) represents the half-plane FW surface current on a finite leading edge incremental strip of length d_l. This incremental strip can be oriented arbitrarily. The relations expressing these PTDEEC's in terms of the FW surface current are readily obtained from the corresponding relations for the first-order PTDEEC's (17)–(18) by introducing a finite upper limit of integration:

$$I_{12}^{\text{ptd}} = \frac{|\hat{u}_l \times \hat{t}_l|}{|\hat{r} \times \hat{t}_l|^2} \hat{r} \cdot (\hat{t}_l \times \hat{r}) \times \int_0^{d_l} \bar{J}_l^{fw}(u_l) \exp(jk\hat{r} \cdot \hat{u}_l u_l)\, du_l \quad (23)$$

$$M_{12}^{\text{ptd}} = \zeta \frac{|\hat{u}_l \times \hat{t}_l|}{|\hat{r} \times \hat{t}_l|^2} \hat{t}_l \cdot \hat{r} \times \int_0^{d_l} \bar{J}_l^{fw}(u_l) \exp(jk\hat{r} \cdot \hat{u}_l u_l)\, du_l. \quad (24)$$

The explicit expressions for these PTDEEC's are found through an evaluation of the integrals (23)–(24) employing the half-plane FW surface current (11)–(12):

$$I_{12}^{\text{ptd}} = (\bar{E}^i \cdot \hat{t}_l) \frac{4e^{-j\pi/4}}{k\zeta\sqrt{\pi}} \frac{\sin\frac{\alpha_l^i}{2}}{\sin\beta_l^i} \left\{ V_2 - 2\cos\frac{\alpha_l^i}{2} V_1 \right\} + (\bar{H}^i \cdot \hat{t}_l) \frac{4e^{-j\pi/4}}{k\sqrt{\pi}} \left\{ (\cot\beta_l^i \cos\alpha_l^i + \cot\beta_l \cos\alpha_l) V_1 - \cos\frac{\alpha_l^i}{2} \cot\beta_l^i V_2 \right\} \quad (25)$$

$$M_{12}^{\text{ptd}} = (\bar{H}^i \cdot \hat{t}_l) \frac{4e^{-j\pi/4}\zeta}{k\sqrt{\pi}} \frac{\sin\alpha_l}{\sin\beta_l} V_1. \quad (26)$$

The term ν_l was defined above (21), and the terms V_1 and V_2 are given by

$$V_1 = \left\{ F\left(\sqrt{2kd_l \sin\gamma_l \sin\beta_l^i}\cos\frac{\alpha_l^i}{2}\right) \exp\left(jkd_l \sin\gamma_l (\sin\beta_l^i \cos\alpha_l^i + \nu_l)\right) - \frac{\sqrt{\pi}}{2} e^{-j\pi/4} + \sin\beta_l^i \cos\frac{\alpha_l^i}{2} V_2 \right\} / (\sin\beta_l^i \cos\alpha_l^i + \nu_l) \quad (27)$$

$$V_2 = \frac{1}{\sqrt{2\sin\beta_l^i}} \begin{cases} \dfrac{\sqrt{\pi} e^{-j\pi/4} - 2F\left(\sqrt{kd_l \sin\gamma_l (\sin\beta_l^i - \nu_l)}\right)}{\sqrt{\sin\beta_l^i - \nu_l}}, & \sin\beta_l^i > \nu_l \\ 2\sqrt{kd_l \sin\gamma_l}, & \sin\beta_l^i = \nu_l \\ \dfrac{\sqrt{\pi} e^{j\pi/4} - 2F^*\left(\sqrt{kd_l \sin\gamma_l |\sin\beta_l^i - \nu_l|}\right)}{\sqrt{|\sin\beta_l^i - \nu_l|}}, & \sin\beta_l^i < \nu_l \end{cases} \quad (28)$$

wherein "*" denotes the complex conjugate. It is observed that the first set of the higher order PTDEEC's (25)–(26) depends on the tangential components of the incident field ($\bar{E}^i \cdot \hat{t}_l$, $\bar{H}^i \cdot \hat{t}_l$), the direction of incidence (α_l^i, β_l^i), the direction of observation (α_l, β_l), the direction of the incremental strip γ_l, and its length d_l. Consequently, when the PTDEEC's are employed in the line radiation integral (16), these parameters must be determined at each element of integration.

An asymptotic expansion of the first set of the higher order PTDEEC's (25)–(26) in the limit $kd_l \to \infty$ is obtained [9] by employing the asymptotic representation of the Fresnel function (13c). The first term in this expansion, of order k^{-1}, equals the first-order PTDEEC's, and thus is associated with the first-order edge diffraction. The second term, of order $k^{-3/2}$, depends only on the tangential component of the incident magnetic field at the leading edge and accounts for part of the second-order edge diffraction.

The singular problems associated with the first-order PTDEEC's (19)–(20), in particular the so-called Ufimtsev singularity [18], have been eliminated from the first set of the higher order PTDEEC's (25)–(26). When these are employed in the line radiation integral (16) and the incremental strip is oriented in the direction of the Keller cone, the calculated field will be finite for all directions of incidence and observation.

The first set of the higher order PTDEEC's (25)–(26) are based on incremental strips of finite length. By using the finite strips rather than the infinite strips underlying the first-order PTDEEC's, the source of error constituted by that part of the infinite strip extending beyond the actual scatterer is eliminated. Michaeli's approach [17] and this approach should thus lead to identical results. However, there are some differences between the two approaches to be noted. First, Michaeli orientates the incremental strip in the direction of the Keller cone prior to the derivation of the PTDEEC expressions, while the PTDEEC expressions (25)–(26) hold for any direction of the incremental strip. However, as in the first-order case, the incremental strip must be oriented in the direction of the Keller cone in numerical calculations. Second, whereas the approach suggested above leads to a set of higher

order PTDEEC's to be applied at the leading edge *instead of* the first-order PTDEEC's, Michaeli's approach introduces a set of second-order PTDEEC's to be applied at the trailing edge, and used *together with* his first-order PTDEEC's [18]. Consequently, the elimination of the Ufimtsev singularity in Michaeli's approach depends on the cancellation of two opposite singularities present in his first and second-order PTDEEC's. In contrast, the Ufimtsev singularity has been removed from the PTDEEC's expressions (25)–(26), and these are thus numerically well behaved. Another consequence is that the determination of the limits of the radiation integral along the trailing edge required by Michaeli's approach is avoided by the approach suggested above.

The approach presented here for the finite leading edge strip, yielding the first set of higher order PTDEEC's (25)–(26), corresponds to the approach by Shore and Yaghjian [8] for ILDC's. In both approaches, the derived expressions represent the half-plane FW surface current on an arbitrarily oriented, finite incremental strip. In both approaches, the Ufimtsev singularity is thus removed from the analytical expressions which are to be integrated along the leading edge. The differences are that the approach herein is formulated in terms of PTDEEC's, while the approach by Shore and Yaghjian is formulated in terms of ILDC's, and that the derivations employed in the two approaches are quite different.

The field produced by the first set of the higher order PTDEEC's will, in most cases, provide a better approximation to the FW field than the field of the first-order PTDEEC's. Nevertheless, it does not account properly for the diffraction at the trailing edge. This is manifest in the approximate surface current represented by the first set of the higher order PTDEEC's: since the half-plane surface current on the leading edge incremental strip is oriented in the direction of the Keller cone, it will have a component normal to the trailing edge, in disagreement with physical considerations. The inclusion of the second set of the higher order PTDEEC's in the next section will eliminate this problem.

V. Second Set of Higher Order PTDEEC's

In order to define the second set of the higher order PTDEEC's, the trailing edge FW surface current $\bar{J}_t^{\mathrm{fw}}$ excited at the trailing edge due to the incident leading edge FW surface current $\bar{J}_l^{\mathrm{fw}}$ must first be determined. In Section II, it was pointed out that for the case of a half-plane illuminated at grazing incidence ($\alpha^i = 0$), the FW surface current excited at the edge can be expressed in terms of the incident PO surface current (14)–(15). This half-plane problem is analogous to the plate problem where the trailing edge FW surface current is excited at the trailing edge due to the incident leading edge FW surface current; see Fig. 3. Consequently, an expression for the trailing edge FW surface current can be obtained by assuming it possesses the same functional dependence on the value of the incident leading edge FW surface current at the trailing edge as the half-plane FW surface

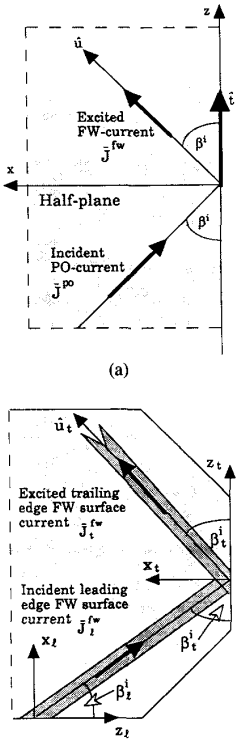

Fig. 3. Analogy between (a) the FW surface current excited at the half-plane edge due to the incident PO surface current associated with a plane wave at grazing incidence, and (b) the trailing edge FW surface current excited at the trailing edge of the actual scatterer due to the incident leading edge FW surface current.

current has on the value of the incident PO surface current at the half-plane edge. The expression for the trailing edge FW surface current along the trailing edge Keller cone is thus obtained from the expressions (14)–(15) by substituting $\bar{J}^{\mathrm{po}}$ and $\bar{J}^{\mathrm{fw}}$ with $\bar{J}_l^{\mathrm{fw}}$ and $\bar{J}_t^{\mathrm{fw}}$, respectively:

$$J_{t,x_t}^{\mathrm{fw}}(u_t) = J_{l,x_t}^{\mathrm{fw}}(u_t = 0)\frac{-2e^{j\pi/4}}{\sqrt{\pi}}F\left(\sqrt{2ku_t}\,\sin\beta_t^i\right) \cdot \exp\left[jku_t(\sin^2\beta_t^i - \cos^2\beta_t^i)\right] \tag{29}$$

$$J_{t,z_t}^{\mathrm{fw}}(u_t) = J_{l,z_t}^{\mathrm{fw}}(u_t = 0)\frac{-2e^{j\pi/4}}{\sqrt{\pi}} \cdot \left\{F\left(\sqrt{2ku_t}\,\sin\beta_t^i\right) - \frac{e^{-j2ku_t\sin^2\beta_t^i}}{j\sqrt{2ku_t}\,\sin\beta_t^i}\right\} \cdot \exp\left[jku_t(\sin^2\beta_t^i - \cos^2\beta_t^i)\right]. \tag{30}$$

It is noted that the components of the FW surface currents appearing in these expressions are the components in the local trailing edge coordinate system. The relations between the components of the leading edge FW surface current in the local trailing and leading edge coordinate

systems are

$$J^{\mathrm{fw}}_{l,x_t}(u_t = 0) = \cos(\beta_l^i + \beta_t^i) J^{\mathrm{fw}}_{l,x_l}(u_l = d_l) - \sin(\beta_l^i + \beta_t^i) J^{\mathrm{fw}}_{l,z_l}(u_l = d_l) \quad (31)$$

$$J^{\mathrm{fw}}_{l,z_t}(u_t = 0) = \sin(\beta_l^i + \beta_t^i) J^{\mathrm{fw}}_{l,x_l}(u_l = d_l) + \cos(\beta_l^i + \beta_t^i) J^{\mathrm{fw}}_{l,z_l}(u_l = d_l) \quad (32)$$

and the value of the leading edge FW surface current at the trailing edge expressed in the leading edge coordinate system is subsequently obtained from the expressions for the half-plane FW surface current (11)–(12). It is noted that the leading edge incremental strip has been oriented along the intersection of the scatterer and the leading edge Keller cone, i.e., $\gamma_l = \beta_l^i$ or $\hat{u}_l = \hat{x}_l \sin\beta_l^i + \hat{z}_l \cos\beta_l^i$.

The analogy applied here is approximate since the leading edge FW surface current does not, in general, possess the characteristics of the PO surface current at grazing incidence on the half-plane. If the argument of the Fresnel function appearing in the expressions for the FW surface current (11)–(12) is large, the FW surface current locally takes the form of the PO surface current: the constant phase contours are parallel straight lines, and the orientation of the current is perpendicular to these, i.e., in the direction of propagation, which also coincides with the intersection of the scatterer and the Keller cone. This is seen by employing the asymptotic representation of the Fresnel function (13c) in the FW surface current expressions (11)–(12). In this case, the analogy is accurate. If the argument of the Fresnel function is small, the FW surface current may not possess the characteristics of the PO surface current, and the analogy may become less accurate. Two important cases leading to a small argument are those in which either the separation between the leading and trailing edges is small, $kd_l < 1$, or the direction of propagation of the incident plane wave is close to edge-on at the leading edge, $\alpha_l^i \approx \pi$. The first case occurs when the leading and trailing edge points are close to a corner of the polygonal plate. Hence, the half-plane modeling of the actual surface current is inherently inaccurate since the corner-excited surface current is not taken into account. Even a more accurate expression for the trailing edge FW surface current would not overcome this problem. In the case of edge-on incidence, the leading edge FW surface current still possesses the characteristics of the PO surface current provided that the incident electric field is perpendicular to the leading edge. If not, the constant phase contours will still be parallel straight lines, but the leading edge FW surface current will possess a component parallel to these, i.e., normal to the direction of propagation. This discrepancy between the leading edge FW surface current and the PO surface current agrees with the nonray-optical behavior of the leading edge diffracted field along the scatterer for edge-on incidence [23]. It is noted that for any separation, for any direction of the incident plane wave, and for any polarization of this, the suggested model will ensure that the component of the leading edge FW surface current normal to the trailing edge is cancelled by a similar but oppositely directed component of the trailing edge FW surface current. This is verified by setting u_t equal to zero in the expression for the trailing edge FW surface current (29).

The second set of the higher order PTDEEC's (I_{23}^{ptd}, M_{23}^{ptd}) represents the trailing edge FW surface current on a finite trailing edge incremental strip of length d_t oriented in the direction of the trailing edge Keller cone and extending from the trailing edge to the third edge (Fig. 1). This second set of the higher order PTDEEC's is defined to be placed at the leading edge. Through identification of the expressions for the far fields produced by the trailing edge FW surface current along the trailing edge incremental strip and the PTDEEC's at the leading edge, it is found [9] that the latter can be related to the former as

$$I_{23}^{\mathrm{ptd}} = \frac{|\hat{k} \times \hat{t}_l|}{|\hat{r} \times \hat{t}_l|^2} \exp(jkd_l \hat{r} \cdot \hat{u}_l) \hat{r} \cdot (\hat{t}_l \times \hat{r}) \times \int_0^{d_t} \bar{J}_t^{\mathrm{fw}} \exp(jku_t \hat{r} \cdot \hat{u}_t)\, du_t \quad (33)$$

$$M_{23}^{\mathrm{ptd}} = \zeta \frac{|\hat{k} \times \hat{t}_l|}{|\hat{r} \times \hat{t}_l|^2} \exp(jkd_l \hat{r} \cdot \hat{u}_l) \hat{t}_l \cdot \hat{r} \times \int_0^{d_t} \bar{J}_t^{\mathrm{fw}} \exp(jku_t \hat{r} \cdot \hat{u}_t)\, du_t. \quad (34)$$

Introducing the trailing edge FW surface current expressions (29)–(30) into the integral expressions (33)–(34), it is found that

$$I_{23}^{\mathrm{ptd}} = V_3 \frac{2e^{-j\pi/4}}{\sqrt{\pi}} \frac{1}{k \sin\beta_t^i} \cdot \Big\{ \big[\cos(\beta_l^i + \beta_t^i) - \cos\beta_l \cos\beta_t\big] J^{\mathrm{fw}}_{l,z_t}(0)(V_5 - V_4) + \big[\sin(\beta_l^i + \beta_t) + \cos\beta_l \sin\beta_t \cos\alpha_t\big] J^{\mathrm{fw}}_{l,x_t}(0) V_4 \Big\} \quad (35)$$

$$M_{23}^{\mathrm{ptd}} = -\zeta V_3 \frac{2e^{-j\pi/4}}{\sqrt{\pi}} \frac{\sin\alpha_l \sin\beta_l}{k \sin\beta_t^i} \cdot \Big\{ \sin(\beta_l^i + \beta_t^i) J^{\mathrm{fw}}_{l,z_t}(0)(V_5 - V_4) - \cos(\beta_l^i + \beta_t^i) J^{\mathrm{fw}}_{l,x_t}(0) V_4 \Big\} \quad (36)$$

wherein the terms V_3, V_4, V_5, and ν_t are given by

$$V_3 = \frac{\sin \beta_l^i}{\sin^2 \beta_l} \exp\left(jkd_l[\sin \beta_l \cos \alpha_l \sin \beta_l^i + \cos \beta_l \cos \beta_l^i]\right) \tag{37}$$

$$V_4 = \left\{F\left(\sqrt{2kd_t} \sin \beta_t^i\right) \exp\left(jkd_t \sin \beta_t^i (\sin \beta_t^i + \nu_t)\right) - \frac{\sqrt{\pi}}{2} e^{-j\pi/4} + \sin \beta_t^i V_5\right\} / (\sin \beta_t^i + \nu_t) \tag{38}$$

$$V_5 = \frac{1}{\sqrt{2 \sin \beta_t^i}} \begin{cases} \dfrac{\sqrt{\pi} e^{-j\pi/4} - 2F\left(\sqrt{kd_t \sin \beta_t^i (\sin \beta_t^i - \nu_t)}\right)}{\sqrt{\sin \beta_t^i - \nu_t}}, & \sin \beta_t^i > \nu_t \\ 2\sqrt{kd_t \sin \beta_t^i} & \sin \beta_t^i = \nu_t \end{cases} \tag{39}$$

$$\nu_t = \sin \beta_t \cos \alpha_t + \cot \beta_t^i (\cos \beta_t - \cos \beta_t^i). \tag{40}$$

The second set of the higher order PTDEEC's depends on the tangential components of the incident field at the leading edge ($\bar{E}^i \cdot \hat{t}_l$, $\bar{H}^i \cdot \hat{t}_l$), the direction of incidence at the leading edge (α_l^i, β_l^i), the direction of observation at the leading edge (α_l, β_l), the length of the leading edge incremental strip d_l, the angle between the leading edge incremental strip and the trailing edge β_t^i, and the length of the trailing edge incremental strip d_t. The angles (α_t, β_t) specifying the direction of observation with respect to the trailing edge point are defined from expressions (6)–(7) with the subscript "l" replaced by "t"; they can also be expressed in terms of the angles already introduced:

$$\cos \beta_t = \sin(\beta_l^i + \beta_t^i) \sin \beta_l \cos \alpha_l + \cos(\beta_l^i + \beta_t^i) \cos \beta_l \tag{41}$$

$$\cos \alpha_t = \frac{1}{\sin \beta_t} \left(\cos(\beta_l^i + \beta_t^i) \sin \beta_l \cos \alpha_l - \sin(\beta_l^i + \beta_t^i) \cos \beta_l\right) \tag{42}$$

$$\sin \alpha_t = \frac{1}{\sin \beta_t} \sin \beta_l \sin \alpha_l. \tag{43}$$

It is noted that the term V_5 (39) has two branches, whereas the corresponding term V_2 (28) of the first set of the higher order PTDEEC's has three. The reason is that while the leading edge incremental strip can be oriented arbitrarily—and thus the term ($\sin \beta_l^i - \nu_l$) can be positive, zero, or negative—the trailing edge incremental strip is fixed in the direction of the trailing edge Keller cone, and thus the term ($\sin \beta_t^i - \nu_t$) cannot take on negative values.

An asymptotic expansion of the second set of the higher order PTDEEC's (35)–(36) in the limit $kd_l \to \infty$ and $kd_t \to \infty$ is obtained [9] by employing the asymptotic representation of the Fresnel function (13c). The first term in this expansion is of order $k^{-3/2}$. It accounts for the remaining part of the second-order edge diffraction, not included in the first set of the higher order PTDEEC's, in the sense that it ensures a zero component of the approximate FW surface current perpendicular to the trailing edge. The second term is of order k^{-2}. This term is due to the finite length of the trailing edge incremental strip, and it accounts for part of the third-order edge diffraction. The sum of the terms of order $k^{-3/2}$ in the asymptotic expansions of the first and second sets of the higher order PTDEEC's should be identical to the asymptotic representation of the second-order PTDEEC's reported by Ivrissimtzis [19].

The only singularity problem associated with the second set of the higher order PTDEEC's occurs when the trailing edge becomes parallel to the leading edge incremental strip, i.e., $\sin \beta_t^i$ goes to zero, and the z_t component of the trailing edge FW surface current (30) become singular. This singularity will also be present in the PTDEEC's (35)–(36) since these then represent an integration of a singular term over a finite region. This is different from the first set of the higher order PTDEEC's which do not become singular as the leading edge becomes parallel to the direction of propagation of the incident plane wave. The difference is caused by the fact that the width of the trailing edge incremental strip is independent of the angle of incidence β_t^i of the incident leading edge FW surface current, whereas the width of the leading edge incremental strip (when this is oriented in the direction of the leading edge Keller cone) is proportional to the sine of the angle of incidence β_l^i. Consequently, whereas the width of the leading edge incremental strip goes to zero at the same rate as the leading edge FW surface current goes to infinity, and the result thus is bounded, the same cancellation will not occur for the trailing edge.

The outlined approach for the inclusion of the second-order edge diffraction differs in several aspects from the four previously reported approaches [8], [17], [19], [20] discussed in Section II. First, Michaeli [17] claimed that the first set of the higher order PTDEEC's will account for the dominant part of the second-order edge diffraction, and consequently ignored the trailing edge FW surface current; i.e., the contribution from the second set of the higher order PTDEEC's (35)–(36) is not included in Michaeli's approach. Second, the EEC's introduced in the three other works [8], [19], [20] were all specified to be placed at the trailing edge. These approaches thus require a determination of those parts of the circumference which are illuminated by other edge elements. By specifying the

EEC's to be placed at the leading edge, such a determination is avoided. Third, the approaches of Ivrissimtzis [19] and Ufimtsev [20] both employ PTDEEC's based on infinite incremental strips at the trailing edge. Consequently, the approximate FW surface current represented by these PTDEEC's exists not only inside, but also outside the area of the actual scatterer; this can cause errors for observation points close to the plane of the scatterer [9]. The approaches of Shore and Yaghjian [8] and this work employ PTDEEC's based on finite incremental strips which limit the extension of the approximate FW surface current to the actual scatterer, and thus avoid this problem. Fourth, the bistatic radar cross section (RCS) of a circular plate has been calculated [9] using the approaches by Shore and Yaghjian, and the present work and comparison were made with an exact solution [24]. It was not possible to conclude whether one of the two approaches in general will provide the most accurate result. However, the differences observed between the two approaches serve to emphasize the importance of an accurate modeling of the second-order edge diffraction.

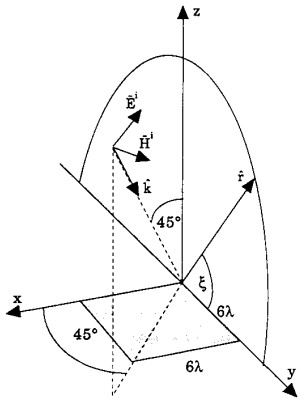

Caustic directions
First-order: ξ= 120°
Second-order: ξ = 30°, 120°, 150°
Third-order: ξ = 30°, 60°, 150°

Fig. 4. Square plate configuration: area = $36\lambda^2$, direction of incidence $(\theta^i, \phi^i) = (45°, 45°)$, plane of observation $\phi = 90°$ or 270°. Directions of observation where caustics of the first-, second-, and third-order edge diffracted rays are present.

VI. Numerical Results

Comparisons between the RCS's predicted by the first-order PTDEEC's (19)–(20) and a combined set of higher order PTDEEC's, obtained by adding the first (25)–(26) and second (35)–(36) sets of the higher order PTDEEC's, have been performed for various configurations [9]. Here, a representative bistatic case is considered. The scatterer is a square plate with corners positioned at $(x, y) = (0, 0)$, $(6\lambda, 0)$, $(6\lambda, 6\lambda)$, and $(0, 6\lambda)$; see Fig. 4. The plane wave, which is linearly polarized along either $\hat{\theta}^i$ or $\hat{\phi}^i$, is incident from the direction $(\theta^i, \phi^i) = (45°, 45°)$. The plane of observation is given by $z \geq 0$ and $\phi = 90°$ or $\phi = 270°$, and the direction of observation is specified by the angle $\xi = \arccos(\hat{r} \cdot \hat{y})$. In this plane of observation, the PO field is zero for all directions of observation.

A radar configuration involving a polygonal scatterer cannot be analyzed by conventional ray-optical techniques since the reflected and edge-diffracted rays form caustics at a few discrete directions of observation and do not exist elsewhere. That is, for any direction of observation, the surface and each of the straight edges possesses either infinitely many or no stationary points. The caustic directions for the first-, second-, and third-order edge-diffracted rays for the present configuration are listed in Fig. 4. The rigorous results included here were calculated by Hansen [25] using a code based on a method of moments (MOM) technique to solve the electric field integral equation. The θ and ϕ components of the RCS, $\sigma_{\theta\theta}$ and $\sigma_{\phi\theta}$, for a θ^i-polarized incident field are shown in Fig. 5(a) and (b), respectively, while the θ and ϕ comonents, $\sigma_{\theta\phi}$ and $\sigma_{\phi\phi}$, for a ϕ^i-polarized incicent field are shown in Figs. 5(c) and (d), respectively. The MOM result is designated MOM, while the first- and higher order PTDEEC results are designated EEC^1 and EEC^2, respectively.

For the first-order result EEC^1, a very good agreement is found for the RCS's $\sigma_{\theta\theta}$ and $\sigma_{\theta\phi}$ in the main lobe in concordance with the presence of first-order diffraction in the direction ξ equal to 120°. Away from this direction, the level predicted by EEC^1 becomes much smaller than that of MOM, while the positions of the side lobes and nulls agree, even at wide angles. Good agreement is also found for the RCS $\sigma_{\phi\theta}$ around the main lobe. However, away from this region, the complicated side lobe structure of the MOM solution is not well approximated by the EEC^1 approach. For the RCS $\sigma_{\phi\phi}$, it is observed that the first-order result does not furnish as good an approximation in the main lobe region as was the case for the other polarizations.

Next, the higher order PTDEEC results are considered. For the RCS $\sigma_{\theta\theta}$, the use of the higher order PTDEEC's has the effect of raising the level in a large region. At the leftmost maximum, ξ close to 30° where second-order diffraction is present, the change amounts to 12 dB. The higher order result has minima which are in better agreement with the MOM solution than the nulls of the first-order results are. For the RCS $\sigma_{\phi\theta}$, the improvements are even more pronounced. In the wide angle regions which contain the two directions, ξ equal to 30° and 150°, at which second-order diffraction effects are present, the level is raised by almost 20 dB, and the pattern is drastically changed from that of the first-order solution. For instance, the zero of the MOM solution at ξ equal to 53° is recovered by the higher order PTDEEC's, whereas the first-order PTDEEC's predict a maximum at this position. Furthermore, the first-order zero at ξ close to 70° is changed by the higher order approach into a local maximum, in accordance with the rigorous solution. For the ϕ^i-polarized incident plane wave, the results parallel qualitatively those observed above for the θ^i-polarized incident field. For the RCS $\sigma_{\phi\phi}$, it is interesting to note that

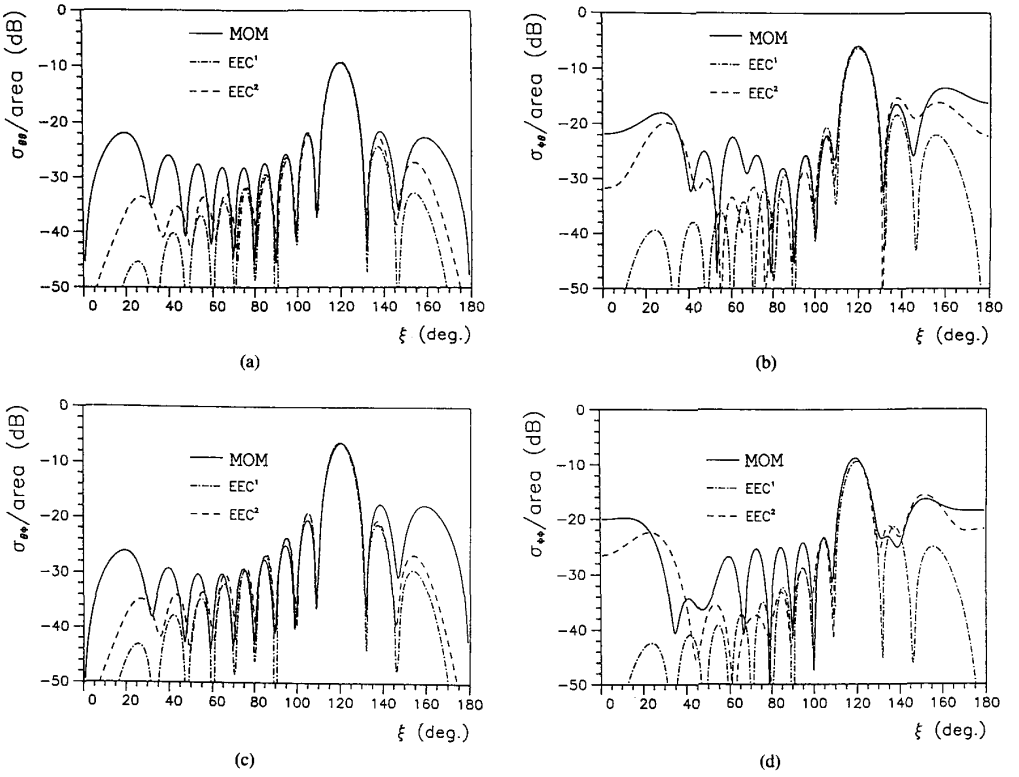

Fig. 5. Normalized RCS for square plate configuration of Fig. 4. MOM: method of moments, EEC[1]: first-order PTDEEC's, EEC[2]: higher order PTDEEC's. (a) $\sigma_{\theta\theta}$. (b) $\sigma_{\phi\theta}$. (c) $\sigma_{\theta\phi}$. (d) $\sigma_{\phi\phi}$.

the discrepancy between the first-order PTDEEC and MOM results in the main lobe is eliminated when the higher order PTDEEC's are employed.

In summary, for the square plate configuration, the approximation is significantly improved when the higher order edge diffraction is taken into account. The major improvements are found in those directions at which it was previously recognized that second-order diffraction effects are present. The remaining discrepancies are caused by effects which are not included in the proposed approach. The most important of these are the edge interaction of higher order than accounted for by the finite trailing edge incremental strip, the slope diffraction at the trailing edge caused by the spatial variation of the field associated with the leading edge FW surface current, and the corner currents, e.g., the edge waves excited at the corners and propagating along the edges. The higher order edge interactions can be incorporated by straightforwardly repeating the approach, leading to the second set of the higher order PTDEEC's. The slope diffraction can be incorporated by deriving the second set of the higher order PTDEEC's on the basis of an expression for the trailing edge FW surface current which accounts for the spatial variation, i.e., the slope, of the field associated with the incident leading edge FW surface current. An inclusion of the edge waves could be accomplished through an extension of the work by Hansen [26], who established expressions for these for the quarter plane and a wide range of directions of incidence.

VII. Conclusion

An approach for including higher order edge diffraction in the EEC method has been proposed. This approach, which applies to mono- and well as bisatic radar configurations with perfectly conducting polygonal plates,involves three distinct sets of EEC's. The first set comprises the POEEC's which yields the same result as obtained from a surface integration over the PO surface current; these POEEC's are not dealt with explicitly herein as an account of these can be found elsewhere [9]. The second set is termed the first set of the higher order PTDEEC's. These PTDEEC's were derived from an integration over the leading edge FW surface current along a finite incremental strip, and these account for the first- and part of the second-order edge diffraction. The third set, referred to as the second set of the higher order PTDEEC's, were derived from an integration over the trailing edge FW surface current along a finite incremental strip. An expression for this surface current was obtained by letting it have the same dependence on the incident leading edge FW surface current as the FW surface current has on the incident PO surface current in the half-plane case with grazing incidence. The second set of the higher order PTDEEC's accounts for the remaining part of the

second-order edge diffraction in the sense that it ensures a zero component of the approximate FW surface current normal to the trailing edge; furthermore, part of the third-order edge diffraction is also accounted for. All of these sets of EEC's contain very few singularity problems. In order to obtain an approximation to the scattered field, the three sets of EEC's are added and integrated along the circumference of the scatterer. This procedure is straightforward, and since most singularity problems have been eliminated from the EEC expressions, it is numerically well behaved. The proposed approach was applied to a configuration involving a square plate. Substantial improvements were achieved by using the higher order PTDEEC's instead of the first-order PTDEEC's. These calculations also illustrated that the edge interaction can be significant, although the direction of incidence is far from the plane of the scatterer. The discrepancies which still remain between the approximate and rigorous results were attributed to higher order edge diffraction than accounted for by the present approach, slope diffraction at the trailing edge and corner diffraction. The possibilities for including these effects in the EEC method were pointed out. Finally, it is noted that the approach can be extended to also apply to polyhedral objects by employing the wedge rather than the half-plane solution in the derivation of the higher order PTDEEC's.

Acknowledgment

The author wishes to thank A. D. Yaghjian for suggesting the use of finite incremental strips, T. B. Hansen for the calculation of the MOM results, and both of them for many valuable discussions. L. P. Ivrissimtzis is acknowledged for his careful review of the original manuscript.

References

[1] R. F. Millar, "An approximate theory of the diffraction of an electromagnetic wave by an aperture in a plane screen," *Proc. IEE*, vol. 103C, pp. 177–185, Mar. 1956.

[2] K. M. Mitzner, "Incremental length diffraction coefficients," Technical Rep. AFAL-TR-73-296, Northrop Corp., Apr. 1974.

[3] A. Michaeli, "Equivalent edge currents for arbitrary aspects of observation," *IEEE Trans. Antennas Propagat.*, vol. AP-32, pp. 252–258, Mar. 1984; and "Corrections to 'Equivalent edge currents for arbitrary aspects of observation,'" *IEEE Trans. Antennas Propagat.*, vol. AP-33, p. 227, Feb. 1985.

[4] R. A. Shore and A. D. Yaghjian, "Incremental diffraction coefficients for planar surfaces," *IEEE Trans. Antennas Propagat.*, vol. 36, pp. 55–70, Jan. 1988; and "Correction to 'Incremental diffraction coefficients for planar surfaces,'" *IEEE Trans. Antennas Propagat.*, vol. 37, p. 1342, Oct. 1989.

[5] T. J. Brinkley and R. J. Marhefka, "Far zone bistatic scattering from flat plates," Tech. Rep. 718295-8, ElectroSci. Lab., The Ohio State Univ., June 1988.

[6] O. Breinbjerg, "Prediction of bistatic scattering from perfectly conducting plates by the method of equivalent edge currents," in *URSI Radio Sci. Meet., Program and Abstr.*, May 1990, p. 390.

[7] A. Sommerfeld, "Mathematische Theorie der Diffraction," *Math. Ann.*, vol. 47, pp. 317–374, 1896.

[8] R. A. Shore and A. D. Yaghjian, "Incremental diffraction coefficients for the truncated half-plane and the calculation of the bistatic radar cross section of the disk," Rep. RADC-TR-89-263, Rome Air Develop. Cen., Hanscom AFB, MA, Oct. 1989; and R. A. Shore and A. D. Yaghjian, "Incremental diffraction coefficients for plane conformal strips with application to bistatic scattering from the disk," *J. Electromagn. Waves Appl.*, vol. 6, no. 3, pp. 359–396, 1992.

[9] O. Breinbjerg, "Equivalent edge current analysis of electromagnetic scattering by plane structures," Ph.D. dissertation LD 83, Electromagn. Inst., Tech. Univ. Denmark, Mar. 1991.

[10] R. F. Millar, "The diffraction of an electromagnetic wave by a circular aperture," *Proc. IEE*, vol. 104C, pp. 87–95, Mar. 1957.

[11] ——, "The diffraction of an electromagnetic wave by a large aperture," *Proc. IEE*, vol. 104C, pp. 240–250, Sept. 1957.

[12] W. D. Burnside and L. Peters, Jr., "Axial-radar cross section of finite cones by the equivalent-current concept with higher-order diffraction," *Radio Sci.*, vol. 7, pp. 943–948, Oct. 1972.

[13] E. F. Knott and T. B. A. Senior, "Second-order diffraction by a ring discontinuity," Rep. AFOSR-TR-73-1237, Radiation Lab., Univ. Michigan, July 1973.

[14] F. A. Sikta, "UTD analysis of electromagnetic scattering by flat plate structures," Ph.D. dissertation, ElectroSci. Lab., The Ohio State Univ., 1981.

[15] D. S. Wang and L. N. Medgyesi-Mitschang, "Electromagnetic scattering from finite circular and elliptic cones," *IEEE Trans. Antennas Propagat.*, vol. AP-33, pp. 488–497, May 1985.

[16] R. G. Kouyoumjian and P. H. Pathak, "A uniform geometrical theory of diffraction for an edge in a perfectly conducting screen," *Proc. IEEE*, vol. 62, pp. 1448–1461, Nov. 1974.

[17] A. Michaeli, "Equivalent currents for second-order diffraction by the edges of perfectly conducting polygonal surfaces," *IEEE Trans. Antennas Propagat.*, vol. AP-35, pp. 183–190, Feb. 1987.

[18] ——, "Elimination of infinities in equivalent edge currents, Part I: Fringe current components," *IEEE Trans. Antennas Propagat.*, vol. AP-34, pp. 912–918, July 1986.

[19] L. P. Ivrissimtzis, "High frequency electromagnetic scattering by conducting polyhedral structures," Ph.D. dissertation, ElectroSci. Lab., The Ohio State Univ., 1990.

[20] P. Ya. Ufimtsev, "Elementary edge waves and the physical theory of diffraction," *Electromagn.*, vol. 11, pp. 125–160, Apr.–June 1991.

[21] A. Michaeli, "Elimination of infinities in equivalent edge currents, Part II: Physical optics components," *IEEE Trans. Antennas Propagat.*, vol. AP-34, pp. 912–918, July 1986.

[22] M. Ando, T. Murasaki, and T. Kinoshita, "Elimination of false singualrities in GTD equivalent edge currents," *Proc. IEE*, part H, vol. 138, pp. 289–296, Aug. 1991.

[23] S. W. Lee, Y. Rahmat-Samii, and R. C. Menendez, "GTD, ray-field, and comments on two papers," *IEEE Trans. Antennas Propagat.*, vol. AP-26, pp. 352–354, Mar. 1978.

[24] D. B. Hodge, "The calculation of far-field scattering by a circular metallic disk," Rep. 710816-2, ElectroSci. Lab., Ohio State Univ., 1979.

[25] T. B. Hansen, "Diffraction by a perfectly conducting square plate," Rep. R 399, Electromagn. Inst., Tech. Univ. Denmark, Aug. 1989.

[26] ——, "Corner diffraction coefficients for the quarter plane," *IEEE Trans. Antennas Propagat.*, vol. 39, pp. 976–984, July 1991.

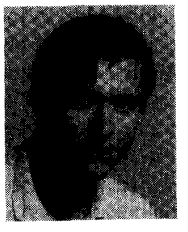

Olav Breinbjerg (M'87) was born in Silkeborg, Denmark, on July 16, 1961. He received the M.S. and Ph.D. degrees in electrical engineering from the Technical University of Denmark, Lyngby, Denmark in 1987 and 1992.

In the Fall of 1988 he was a Visiting Research Scientist at the Electromagnetics Directorate of Rome Air Development Center, Hanscom Air Force Base, MA. From 1989 to 1991 he was a Research Associate at The TUD–ESA Spherical Near-Field Antenna Test Facility, Lyngby, Denmark. Since 1991 he has been an Assistant Professor at the Electromagnetics Institute, Technical University of Denmark. His major research is in high-frequency techniques for electromagnetic scattering analysis in relation to RCS and antenna problems.